NEOPLASIA
www.neoplasia.com
Volume 23 Number xxx Month 2021 pp. 898–911

Original Research

Trop-2 induces ADAM10-mediated cleavage of E-cadherin and drives EMT-less metastasis in colon cancer

Emanuela Guerra[a,b,†]; Marco Trerotola[a,b,†]; Valeria Relli[a,c]; Rossano Lattanzio[a,d]; Romina Tripaldi[a]; Giovanna Vacca[a]; Martina Ceci[a]; Khouloud Boujnah[e]; Valeria Garbo[e]; Antonino Moschella[e]; Romina Zappacosta[a]; Pasquale Simeone[a,#]; Robert de Lange[f]; Ulrich H. Weidle[f]; Maria Teresa Rotelli[g]; Arcangelo Picciariello[g]; Raffaella Depalo[h]; Patrizia Querzoli[i]; Massimo Pedriali[j]; Enzo Bianchini[l]; Domenico Angelucci[k]; Giuseppe Pizzicannella[l]; Carla Di Loreto[m]; Mauro Piantelli[a,b]; Laura Antolini[n]; Xiao-Feng Sun[o]; Donato F. Altomare[f,g]; Saverio Alberti[a,c,e,*]

[a] Laboratory of Cancer Pathology, Center for Advanced Studies and Technology (CAST), "G. d' Annunzio" University of Chieti-Pescara, 66100 Chieti, Italy
[b] Department of Medical, Oral and Biotechnological Sciences, "G. d'Annunzio" University of Chieti-Pescara, 66100 Chieti, Italy
[c] Oncoxx Biotech, 66034 Lanciano (Chieti), Italy
[d] Department of Innovative Technologies in Medicine & Dentistry, 'G. d'Annunzio' University of Chieti-Pescara, 66100 Chieti, Italy
[e] Unit of Medical Genetics, Department of Biomedical Sciences - BIOMORF, University of Messina, 98125 Messina, Italy
[f] Roche Diagnostics GmbH, Pharma Research, D-82372 Penzberg, Germany
[g] General Surgery and Liver Transplantation Unit, Department of Emergency and Organ Transplantation, University 'Aldo Moro', 70124 Bari, Italy
[h] Oncologic Institute IRCCS "Giovanni Paolo II, 70124 Bari, Italy
[i] Section of Anatomic Pathology, Department of Morphology, Surgery and Experimental Medicine, University of Ferrara, 44121 Ferrara, Italy
[j] Operative Unit of Surgical Pathology, University Hospital, 44124 Ferrara, Italy
[k] Department of Pathology, Chieti Hospital, 66100 Chieti, Italy
[l] Department of Pathology, ASL2 Chieti-Lanciano-Vasto, 66100 Chieti, Italy
[m] Department of Pathology, University of Udine, 33100 Udine, Italy
[n] Department of Clinical Medicine,Center for Biostatistics, Prevention and Biotechnology, University of Milano-Bicocca, 20900 Monza, Italy
[o] Department of Oncology, and Department of Biomedical and Clinical Sciences Linköping University, SE-581 85 Linköping, Sweden

Abstract

We recently reported that activation of Trop-2 through its cleavage at R87-T88 by ADAM10 underlies Trop-2–driven progression of colon cancer. However, the mechanism of action and pathological impact of Trop-2 in metastatic diffusion remain unexplored.

Abbreviations: CF, change factor; Δcyto, cytoplasmic-tail deletion mutant; ΔHIKE, HIKE deletion mutant; EMT, epithelial-mesenchymal transition; GFP, green fluorescent protein; IHC, immunohistochemistry; mAb, monoclonal antibody; SC, subcutaneous; SV, voxels.

* Corresponding author.
E-mail address: salberti@unime.it (S. Alberti).
† These authors contributed equally.
# Present address: Laboratory of Cytomorphology, Center for Advanced Studies and Technology (CAST), Department of Medicine and Aging Sciences, "G. d'Annunzio" University of Chieti-Pescara, 66100 Chieti, Italy
Received 30 June 2021; accepted 2 July 2021

https://doi.org/10.1016/j.neo.2021.07.002

Through searches for molecular determinants of cancer metastasis, we identified *TROP2* as unique in its up-regulation across independent colon cancer metastasis models. Overexpression of wild-type Trop-2 in KM12SM human colon cancer cells increased liver metastasis rates *in vivo* in immunosuppressed mice. Metastatic growth was further enhanced by a tail-less, activated ΔcytoTrop-2 mutant, indicating the Trop-2 tail as a pivotal inhibitory signaling element. In primary tumors and metastases, transcriptome analysis showed no down-regulation of *CDH1* by transcription factors for epithelial-to-mesenchymal transition, thus suggesting that the pro-metastatic activity of Trop-2 is through alternative mechanisms. Trop-2 can tightly interact with ADAM10. Here, Trop-2 bound E-cadherin and stimulated ADAM10-mediated proteolytic cleavage of E-cadherin intracellular domain. This induced detachment of E-cadherin from β-actin, and loss of cell-cell adhesion, acquisition of invasive capability, and membrane-driven activation of β-catenin signaling, which were further enhanced by the ΔcytoTrop-2 mutant. This Trop-2/E-cadherin/β-catenin program led to anti-apoptotic signaling, increased cell migration, and enhanced cancer-cell survival. In patients with colon cancer, activation of this Trop-2–centered program led to significantly reduced relapse-free and overall survival, indicating a major impact on progression to metastatic disease. Recently, the anti-Trop-2 mAb Sacituzumab govitecan-hziy was shown to be active against metastatic breast cancer. Our findings define the key relevance of Trop-2 as a target in metastatic colon cancer.

Neoplasia (2021) 23, 898–911

Keywords: E-cadherin, β-catenin, Trop-2, proteolytic cleavage, Metastasis, Signaling networks, Epithelial-mesenchymal transition

Introduction

Metastatic disease is the dominant cause of death in cancer patients, and is the greatest hurdle for cancer cure. Hundreds of proteins/genes have been linked to the metastatic phenotype [1]. However, neither proteomic analysis nor large-scale genome sequencing [2] succeeded in identifying reproducible markers of tumor aggressiveness and metastasis in cancer patients.

Metastasis-associated genes include not only drivers of the metastatic phenotype, but also secondary events, together with adaptive, counterbalancing changes [3]. Thus, to identify candidates with a decisive role in metastatic diffusion, we looked for genes that were concordantly dysregulated across multiple cancer metastasis models. This led to the discovery that *TROP2* is a unique upregulated gene in metastatic colon cancer prototypes. Trop-2 is a tumor and stem cell growth inducer [4-6]. We and others showed that Trop-2 drives liver colonization of prostate cancer cells [7, 8]. Additional findings showed that Trop-2 expression associates to increased *in vitro* migration and invasion of oral squamous cell and gallbladder carcinoma cell lines [9, 10]. Trop-2 was also reported to be associated to altered expression of markers of epithelial-mesenchymal transition (EMT) in stomach and breast cancer [11, 12].

We recently discovered that proteolytic activation of Trop-2 by ADAM10 underlays its capacity to drive colon cancer malignant progression [13]. However, Trop-2-driven mechanisms of action and activatory pathways in metastasis remained unknown. We previously showed that Trop-2 is upregulated upon tumor progression in colon cancer [6]. Here we find that impairment of the membrane-to-nucleus signaling by removal of the Trop-2 cytoplasmic tail boosted the liver metastasis rate and stimulated colorectal cancer growth. NGS and targeted gene-expression profiling showed no increase in EMT transcription factors nor downregulation of the E-cadherin-encoding *CDH1* gene. We found instead that Trop-2 triggered ADAM10 to cleave E-cadherin, leading to release from the scaffolding cytoskeleton, with disruption of cell-cell junctions, acquisition of invasive capability and activation of pro-metastatic signaling by β-catenin.

This Trop-2-driven metastasis program was found to associate to a significantly worse relapse-free and overall survival of patients with colorectal cancer, suggesting a pivotal impact on colorectal cancer progression. Sacituzumab govitecan-hziy is an anti-Trop-2 antibody-SN-38 drug conjugate, which was shown to be effective in metastatic breast cancer [14-17] and was granted accelerated FDA approval as Trodelvy, for use in the clinics. Our findings support an indication for Trop-2-targeting therapies in metastatic colon cancer.

Materials and methods

Cells

The KM12C, KM12SM and KM12L4A human colon carcinoma cell lines were obtained from I. J. Fidler, M. D. Anderson Cancer Center. The KM12SM and KM12L4A were derived from the non-metastatic KM12C, by in vivo selection for acquisition of metastatic ability [18]. The HCT116 and HCT116U5.5 human colon carcinoma cell lines [19] were obtained from Roche Diagnostics GmbH (Penzberg, Germany). The HCT116U5.5 clone was derived from the non-metastatic HCT116, by in vivo selection for acquisition of metastatic ability [19]. Trop-2 low and Trop-2high subpopulations were derived from the parental HT29 colon cancer cell line by fluorescence-activated cell sorting. Frozen master stocks were prepared for each cell line within the first two months from receipt. Experiments were performed on cells that had been resuscitated from master stocks and passaged for no more than 6 months. Cell cultures were periodically checked for absence of mycoplasma contamination by PCR analyses and DAPI staining. The IGROV-1, HT29, HCT116 and KM12 cells were maintained in RPMI 1640 medium with 10% or 20% FBS respectively, sodium pyruvate, non-essential amino acids, L-glutamine and vitamins (Invitrogen). Murine MTE 4-14 cells [13] were grown in DMEM with 10% FBS. Lipofectamine 2000 or LTX (Invitrogen) were used for DNA transfection. Stable transfectants were selected with G-418 and enriched for expression as described [6].

Coimmunoprecipitation and Western blotting

Coimmunoprecipitation was performed as described [7]. Cell lysates and coimmunoprecipitates were analyzed as previously described [20]. Blots were incubated with relevant primary antibodies (as detailed in Supplementary Methods) in Tris-buffered saline and 5% non-fat dry milk. Hybridized filters were washed in TBS, 0.1% Tween-20. Antibody binding was revealed by chemiluminescence, using horseradish-peroxidase-conjugated anti-mouse

(#401215; Calbiochem), anti-rabbit (sc-2004; Santa Cruz Biotechnology) or anti-goat (sc-2020; Santa Cruz Biotechnology) pAbs. Cleavage of E-cadherin was assessed by comparing the signals from the antibodies recognizing the extracellular and intracellular domains of human E-cadherin. Ponceau red staining was routinely used as control of protein loading [21]. Signal intensity was quantified with ImageJ 1.47, using as reference a Kodak gray-scale standards power curve.

Cell aggregation

Cells at 70-90% confluence were detached from tissue culture plates and seeded in low-attachment plates to minimize interference by substrate binding [22]. Cell aggregation was assessed after 1h and 24h incubation at 37°C. Aggregates were quantified by image analysis.

Invasion assay

Inverse matrigel invasion assay was carried out as described in [23]. Briefly, 100 μl of a matrigel/serum-free medium mixture (1:1) was pipetted into Transwell inserts in a 24-well tissue culture plate and incubated for 30 min at 37°C for settling. Then, the Transwell inserts were inverted and 100 μl of cell suspension (containing 10,000 cells) was pipetted onto the filter. Inverted plates were incubated for 4h to allow for cell attachment. The plate was then turned right-side-up and each Transwell insert placed in a well containing serum-free medium. Complete medium was gently pipetted on top of the set matrigel and incubated for 5 d at 37°C. Transwell inserts were placed in fresh 24-well dishes containing 1 ml of 4 μM Calcein AM stain solution. Additional 300 μl of Calcein AM solution was pipetted on top of each filter. After 1h of incubation at 37°C, cells were imaged by confocal microscopy with a 20x objective with optical Z-sections scanned at 15-μm intervals moving up from the underside of the filter into the matrigel.

β-catenin reporter assays

KM12C and KM12SM cells were co-transfected with the β-catenin reporter pTOPFLASH-EGFP (a kind gift from Prof. Rolf Kemler) and plasmids encoding for wtTrop-2, ΔcytoTrop-2 or with control empty vectors. At 48 hours after transfection cells were detached and stained with the T16 anti-Trop-2 mAb conjugated with Alexa-633 for 20 min at 4°C. GFP and Trop-2 expression were analyzed by flow cytometry.

Flow cytometry

Cell analyses and sorts were performed as described [24] (FACSCalibur, FACSCanto II, FACSAria III flow cytometers/cell sorters BD Biosciences). Subtraction of cell autofluorescence and displacement in the red channel were performed for Alexa488-stained cells [6].

Pre-clinical models

KM12 cell transfectants were injected in the spleen of 8-week old female athymic Crl:CD1-Foxn1^{nu} mice (Charles River Laboratories). After 4 weeks mice were euthanized; tumor growth and diffusion to the liver or other organs were determined. All autoptic samples underwent microscopy histopathology analysis to detect minimal primary tumor or metastatic burdens.

Pre-clinical protocols were approved by the Italian Ministry of Health (Prog. 19, 2006) and by the Interuniversity Animal Research Ethics Committee (CEISA) of Chieti-Pescara and Teramo Universities (Prot.26/2011/CEISA/PROG/16).

Patients

IHC analysis for Trop-2 expression was performed on normal colon mucosa, colon cancer and colon cancer metastases. Trios of normal tissue, primary tumor, and metastasis from individual patients bearing breast, uterus, ovary, or colon cancers were analyzed by cDNA RT-PCR/dot blot assay. Kaplan-Meier curves and Cox proportional hazard models were utilized to quantify impact on relapse-free and overall survival of cancer patients.

Studies on human tumor samples were approved by the Italian Ministry of Health (RicOncol RF-EMR-2006-361866, 2006) and by the ethical committee of the University of Regensburg (Germany).

Statistical analyses

Normality of distribution of assay values was verified (www.graphpad.com). Student t-test was utilized for comparison between protein level means between experimental groups. Two-tailed Fisher exact test was utilized to compare tumor take rates and metastasis frequency. Spleen primary tumors and liver metastasis parameter counts (pseudo-glandular differentiation, mitotic figures and apoptotic bodies) were displayed graphically through boxplot representations. Equality of distributions was tested by the Wilcoxon rank sum test, adjusting the significance level for multiple comparisons by the Bonferroni correction (0.05/2).

RESULTS

Transcriptome profiling of metastatic colon cancer cells

To identify drivers of metastatic diffusion, we profiled transcriptomes of unrelated cancer-metastasis systems, in a quest for concordantly dysregulated genes. To date, candidate metastasis genes primarily originated from mouse tumor models [25]. Hence, we focused on human metastatic cancer systems. Two independent human colon cancer metastatic models were analyzed, i.e. the non-metastatic HCT116 versus metastatic HCT116U5.5 cells [19] and the non-metastatic KM12C versus metastatic KM12SM and KM12L4A cells [18]. The HCT116U5.5 metastatic clone was derived from lung metastases of subcutaneously (SC) injected HCT116 cells [19]. Metastatic KM12SM and KM12L4A cells were derived from liver metastases of KM12C cells injected in the mouse spleen [18]. DNA microarray analysis for the expression of 12652 genes in the HCT116 and KM12 metastatic models, identified 70 and 159 differentially expressed genes, respectively (Supplementary Results, Table S1). The intersection of these independent datasets showed predominant, mutually-exclusive expression changes (Fig. 1*A*), indicating widely divergent transcriptomic scenarios in the two colon cancer models. Only two genes, *TROP2/TACSTD2* and *VIMENTIN*, were upregulated in both systems (Fig. 1*A,* Table S1), first suggesting that pro-metastatic programs may only require few decisive determinants. mRNA findings were validated by RT-PCR (Fig. 1*B*). Differential expression of the encoded proteins was validated by Western blotting (Fig. 1*B*), immunofluorescence confocal microscopy and immunohistochemistry (IHC) (Fig. 1*C*).

The role of Trop-2 in metastatic diffusion

Trop-2 proteolytic cleavage by ADAM10 at R87-T88 is required for activation as a driver of primary tumor growth and malignant progression [13], while a two-step A187-V188 and G285-V286 intramembrane proteolysis releases the Trop-2 intracellular tail, which then co-translocates with ß-catenin to the nucleus [4]. To dissect the contribution of Trop-2 nuclear signaling to colon cancer metastasis we designed a membrane-anchored mutant of Trop-2 devoid of the cytoplasmic tail (ΔcytoTrop-2). wtTrop-2 and ΔcytoTrop-2 KM12SM cells were selected by flow cytometry for membrane expression levels comparable to those found in human cancer

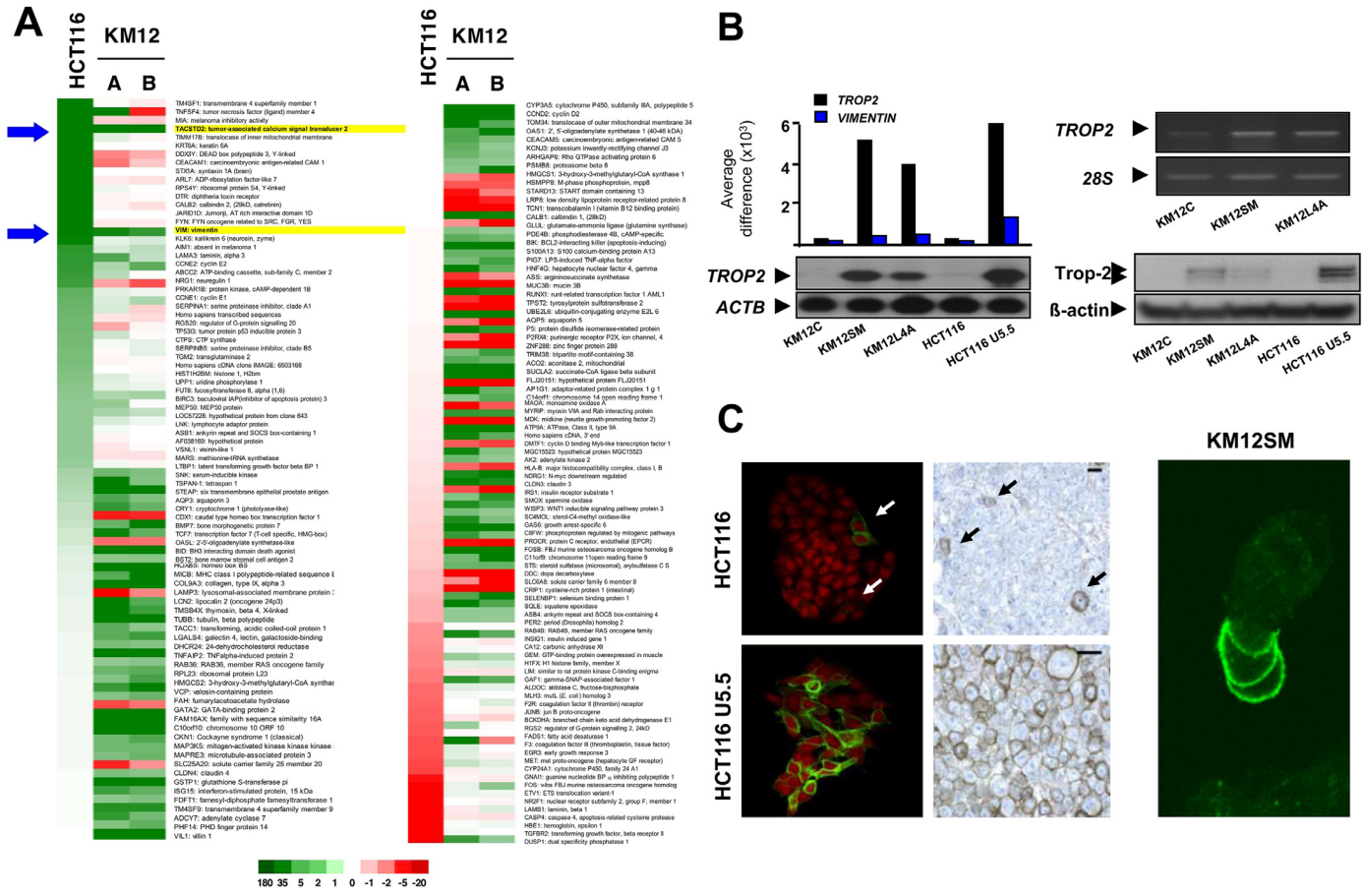

Fig. 1. Transcriptome profiling of metastatic colon cancer cells. (*A*) Transcriptome profiling of metastatic colon cancer cells: HCT116U5.5 vs HCT116 (HCT column) and KM12L4A (A) or KM12SM (B) vs KM12C (KM12 columns). The profiles of the two independent colon cancer metastatic models showed largely mutually exclusive expression changes, indicating widely divergent transcriptomic scenarios. Pseudo-color-coded change factors (CF), according to the scale bar (green, increased expression in metastatic cells; red, decreased expression; white, no change). Genes are sorted by descending CF values in HCT116 cells. Yellow highlight: only two genes, *TROP2/TACSTD2* and *VIMENTIN*, were upregulated in both systems. (***B***) Expression levels of *TROP2* mRNA in KM12C and HCT116 versus KM12SM, KM12L4A or HCT116-U5.5 colon cancer cells. DNA microarray and Northern blot (*left*), and RT-PCR (*upper right*) analyses, with *ACTB* and 28S as loading controls. Western blot analysis (*lower right*) for corresponding Trop-2 protein expression were also performed, with β-actin as loading controls. (***C***) IHC and immunofluorescence assessment of Trop-2 expression in KM12SM and HCT116 U5.5 versus HCT116 colon cancer cells (arrows). Size bars: 50 μm.

(Fig. S1) [6]. KM12SM transfectants were then assayed for capacity to metastasize to the liver upon injection in immunosuppressed mouse spleen (Figure S1) [18]. wtTrop-2 strikingly increased the metastatic capacity of KM12SM cells, raising metastasis rates from 45% for control cells to 90% for wtTrop-2 transfectants (Fig. 2*A*, Table 1, Table S2*A*). The tail-less ΔcytoTrop-2 boosted metastatic growth, with metastatic livers reaching up to four times their normal size at four weeks after tumor injection (3.25± 0.64 cm3 versus 0.45 ± 0.18 cm3 for wtTrop-2, P<0.0001) (Fig. 2*A*, Table 1, Table S2*A*).

Histopathology analysis showed patterns of tumor growth of parental KM12SM cells as manifo.ld nodules, with central necrosis and peripheral fibrous capsule. Residual tumor differentiation capacity was demonstrated by gland rudiments containing apoptotic bodies in their lumen. This closely mirrored human colon cancer, where such crypt-like architecture associates with low cancer grading and good prognosis [26] (Fig. 2*B*, Fig S1, Table S2*B*). wtTrop-2-expressing metastases showed much reduced numbers of differentiated glands (mean±SD glands/20x field: 0.9 ± 0.97 versus 3.42 ± 0.86 in controls, $P = 0.0003$). Poorly differentiated, smaller crypts were also reduced in frequency (2.54 ± 2.33 versus 10.58 ± 7.33 in controls, $P = 0.0026$). Thinner peri-metastatic capsule and pseudo-capsule and frequent mitotic figures (mean±SD mitotic figures/20× field 10.98 ± 9.18 versus 1.58 ± 2.11 in controls, $P = 0.0004$) were observed (Figs. 2*B-C*, Figure S*1,* Table S2*B*). Augmented vascular invasion capacity was also observed (Fig. 2*B*). Loss of central-nodule apoptosis, and a shift toward smaller and peripheral necrotic areas, indicated a reduced apoptotic response to oxygen gradients/distance from blood vessels [27,28] (Figs. 2*B-C,* Table S2*B*).

ΔcytoTrop-2 induced dramatic changes toward invasive growth patterns, with further loss of differentiated glands (0.12 ± 0.32, $P < 0.00001$ versus control) and poorly differentiated glands (1.72 ± 1.44, $P = 0.0007$ versus control) (Fig. 2*B*, Fig. S*1,* Table S2*B*). Frequent mitotic figures were found (5.34 ± 4.39, $P = 0.022$ versus control) (Fig. 2*C*, Fig. S1, Table S2*B*). Cancer cell invasion was detected across layers of hepatocytes or even within pre-existing metastatic areas (Fig. 2*B*), with patterns of invasive growth and little, if any, pseudo-capsule formation. Haemorrhagic necrosis indicated damage to vascular walls. Trop-2-dependent metastases showed diminished apoptotic features in activated ΔcytoTrop-2 versus parental KM12SM cells (mean±SD apoptotic bodies/20x field: 6.92 ± 5.36 versus 13.16 ± 12.75, respectively) (Fig. 2*C*, Fig. S1, Table S2*B*).

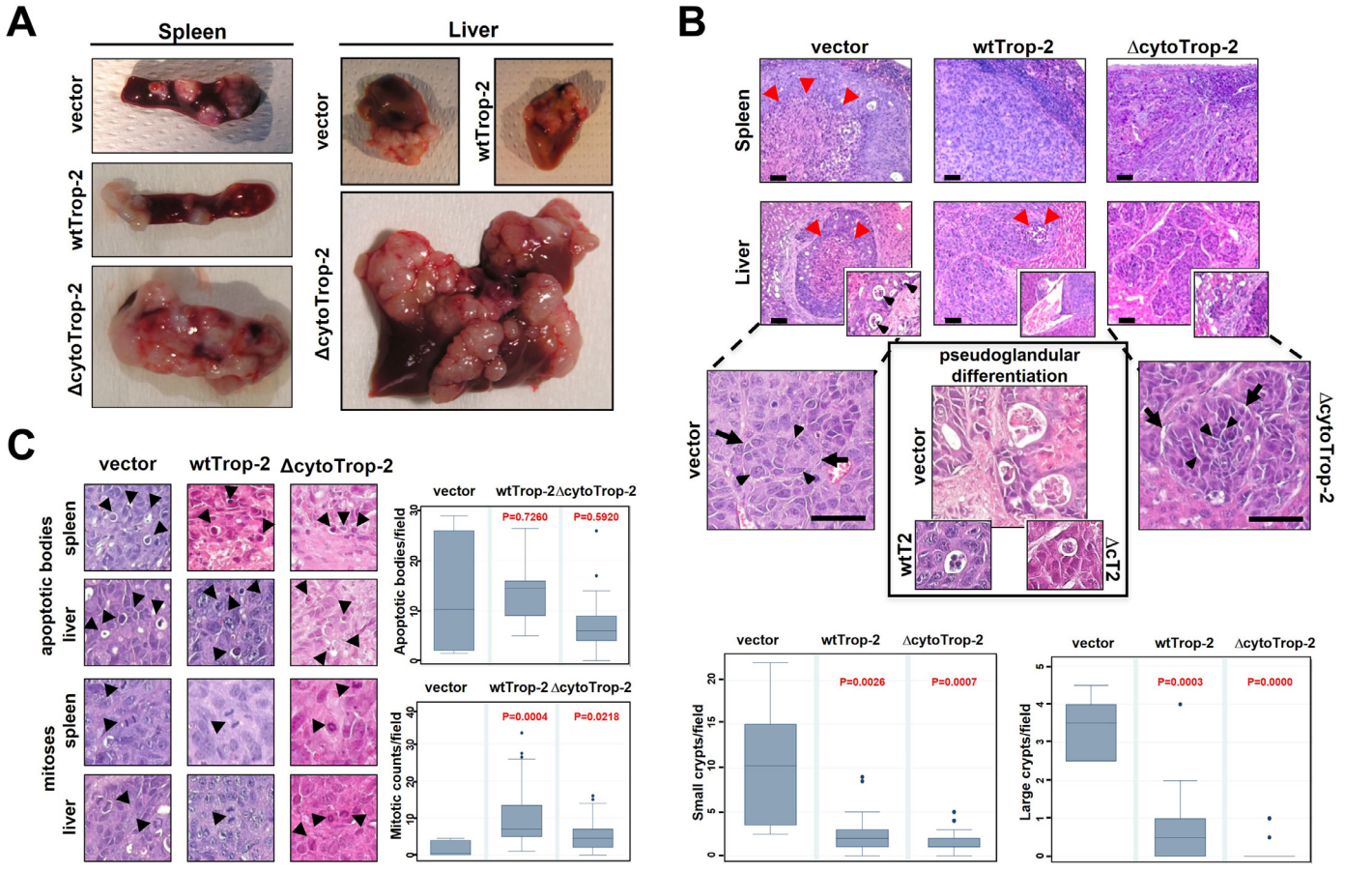

Fig. 2. Trop-2 drives metastasis in vivo. (***A***) Primary spleen tumors and metastatic livers from nude mice injected intra-spleen with KM12SM cells transfected with vector alone, wtTrop-2 or ΔcytoTrop-2. Representative images are shown, full data analysis is in Table S2A. (***B****, top*) Histopathology analysis of spleen and liver tumors from KM12SM transfectants. Control KM12SM/vector cells (left), with central necrotic areas (red arrowheads), defined fibrous capsules and glandular lumen rudiments with apoptotic bodies (*inset*, black arrowheads); KM12SM/wtTrop-2 (*middle*), showing a pleomorphic appearance, numerous mitotic figures and lesser necrosis compared with vector-alone (red arrowheads) and instances of endoluminal vascular growth (*bottom panel, inset*); ΔcytoTrop-2 induced further loss of differentiation: KM12SM/ΔcytoTrop-2 (right), showing an invasive growth pattern (*bottom panel, inset*), frequent mitoses and peripheral haemorrhagic necrosis. (***B***, *bottom*) Decreased cell-cell adhesion in liver metastases from KM12SM/ΔcytoTrop-2 (right) compared to liver metastases from KM12SM/vector cells (left) (arrows). Nodular growth borders are indicated by arrowheads. A representative image of the extent of pseudoglandular differentiation in parental (vector), wtTrop-2 (wtT2), ΔcytoTrop-2 (ΔcT2) cells is shown in the central panel, with data analysis as distribution boxplots of small and large gland-like structures shown below. (***C)*** Spleen tumors and liver metastases from control parental KM12SM, wtTrop-2 and ΔcytoTrop-2 were scored for occurrence of apoptotic bodies (*top*) and mitotic figures (*bottom*) (arrowheads). Representative images are shown on the left, with data analysis as distribution boxplots shown on the right. Tissue sections were stained with haematoxylin and eosin. Size bars = 50 μm. Individual counts for psuedoglandular structures, apoptotic bodies and mitotic counts were obtained per independent 20x optical field and are listed in Table S2*B*. Statistical analysis was conducted as in Material and Methods. Vector: n = 6; wtTrop-2: n = 25; ΔcytoTrop-2: n = 35.

Table 1

***In vivo* metastatic capacity of colon cancer cells expressing Trop-2.**

	% spleen[a]	size (cm^3)	% liver[b]	size (cm^3)
vector	64.9 ± 8.7	0.11 ± 0.04	45.8 ± 14.8	0.50 ± 0.21
wtTrop-2	69.0 ± 10.6	0.09 ± 0.03	**90.0 ± 12.0**[c]	0.45 ± 0.18
ΔcytoTrop-2	**100.0 ± 0**[d]	**0.37 ± 0.23**[e]	76.9 ± 11.7	**3.25 ± 0.64**[f]

vector: *n* = 37; wtTrop-2: *n* = 31; ΔcytoTrop-2: *n* = 13.
Data were from 3 to 9 experiments per group. Values are expressed as mean±SEM. Bold: statistical significance or trend.
[a] primary tumors take rates (percentage of injected cases).
[b] percent incidence of liver metastases.
[c] Fisher's exact test: *P* = 0.0114 versus vector.
[d] Fisher's exact test: *P* = 0.0382 versus wtTrop-2.
[e] trend.
[f] Student's t test: P <0.0001 versus wtTrop-2.

Trop-2 prompted cancer cell rounding and diminished cell-cell adhesion in primary tumors and metastases (Fig. 2*B, bottom panels;* Fig. S*1*).

Profiling of metastatic transcriptomes

NGS transcriptome analysis was conducted on independent KM12SM colon primary tumors and metastases (Figure S1), to detect Trop-2-driven, differential expression of pro-metastatic determinants (Fig. S2). Compound EST analysis showed high intra-group R correlation coefficients, with robust segregation of parental cells, wtTrop-2 and ΔcytoTrop-2, primary cancer and metastasis expression profiles. Sequence alignment over *Mus musculus* or *Homo sapiens* reference genomes formally discriminated transcripts of human cancer origin versus murine stromal components (Table S*3*).

Human EST profiles of primary tumors showed invariant expression of 87.1% of 15782 transcripts between wtTrop-2-expressing versus parental cells. On the other hand, only 19.2% mRNA expression patterns overlapped in wtTrop-2 and control liver metastases, indicating that Trop-2 induces a distinct pro-metastatic program (Fig. S2*A*, Table S3). Wide modulation of the E-cadherin/ß-catenin/TCF-LEF and Wnt/Frizzled/DVL1/APC/ß-catenin pathway components was found, suggesting these to be drivers of Trop-2-induced metastasis. Modulated downstream targets included apoptosis regulators, such as PI3K/Akt [27], NFkB [28], p53 [29], cFOS, caspases 3 and 9, JAK/STAT1-3 and Cyclin D1 [28] (Fig. S2*B*).

Canonical EMT models predict progression to a metastatic state through loss of epithelial differentiation, via transcriptional downregulation of epithelial determinants, such as E-cadherin [1,2,30-32]. Hence, we explored EMT drivers versus epithelial differentiation markers in Trop-2-driven metastatic cells (Table S3*H*). Of 203 EMT biomarkers, 129 were transcribed in the colon cancer cells, 16 were differentially modulated by wtTrop-2/ΔcytoTrop-2; 164 biomarkers were expressed in the tumor stroma, 76 of these were differentially modulated by wtTrop-2 and ΔcytoTrop-2. The EMT transcription factors TWIST1, TWIST2, ZEB1, ZEB2, SNAI2, KLF8, PRRX1, GSC, SIX1 and TCF4 were absent from Trop-2-driven colon cancer cells, SNAI2 was only expressed by the cancer stroma. TFAP2A and TCF3 were downregulated by wtTrop-2 in metastases. (Table S3*H*). Vimentin was not upregulated in metastatic colon cancer cells, but was induced by ΔcytoTrop-2 in stromal cells, consistent with a model whereby the metastasis stroma contributes to global EMT shifts [2].

Among epithelial differentiation determinants, *MAPK6, EPCAM/TACSTD1/TROP1* [33] and most keratins were expressed at comparable levels in primary tumors and metastases. *KRT80*, which is associated with progression of colon cancer, was downregulated by wtTrop-2 in metastases (Table S3*H*). None of the α-integrins, including α6, nor the β-integrins, among them β1, β3, were significantly modulated in cancer cells or stroma. Myosins/β-actin are dynamically co-recruited at the cell membrane upon cross-linking with anti-Trop-2 antibodies. Consistent with this, numerous myosin isoforms were differentially modulated in metastases, whether in stroma (Myo 1a, 1b, 1c, 1f, 1g, H11, L9) or in cancer cells (Myo5a, 6, 7, 10, HC7B, HC10, HC15, myosin regulatory light chain - MRLC2). Conserved, high levels of *CDH1* mRNA were revealed in metastases from wtTrop-2 and ΔcytoTrop-2 versus vector-transfected KM12SM cells as well as in primary tumors across all experimental groups (Table S3*H*). RT-PCR, FACS and Western blotting analyses also showed invariant levels of E-cadherin transcript and protein across transfectants and between control Trop-2-nil/non-metastatic KM12C and Trop-2-low/pro-metastatic KM12SM cells (Figs. S3*A-B, D*).

Taken together these data suggested limited impact of Trop-2 on epithelial differentiation, at variance with previous, more limited analyses [11,12].

Trop-2 releases E-cadherin from the β-actin cytoskeleton and activates ß-catenin

Our findings showed that Trop-2 impacts on the E-cadherin/ß-catenin pathway in metastasis (Figs. S2*B,* Table S3*H*). Evidence of Trop-2-associated reduction in cell-cell adhesion had been obtained by morphometric analysis of metastases growing *in vivo.* Together, these findings suggested a regulatory function of Trop-2 on intercellular junctions via alternative mechanisms to *CDH1* downregulation.

Coimmunoprecipitation assays revealed that wtTrop-2 tightly interacts with E-cadherin (Fig. 3*A*). ΔcytoTrop-2 bound E-cadherin to a lesser extent, first suggesting a role of the Trop-2 cytoplasmic tail in macromolecular assembly with E-cadherin. We thus hypothesized an antagonistic function of Trop-2 versus E-cadherin/ß-catenin-mediated cell-cell adhesion that would critically contrbute to metastatic diffusion [34]. This was explored in *in vitro* assays on low cell-attachment substrates. wtTrop-2 and ΔcytoTrop-2 markedly diminished KM12SM cell-cell adhesion (Fig. 3*C*). Distribution profiles of wtTrop-2 /ΔcytoTrop-2 cells indicated a highly significant reduction in aggregates with respect to control cells (χ2 test P-value <2.2e−16). A shift of aggregate cluster size, toward smaller cell clusters and isolated cells, was correspondingly observed (Fig. 3*C*). Corresponding invasive capability of KM12SM transfectants was assesses by inverse matrigel invasion assays [35]. wtTrop-2 expression conferred KM12SM cells the ability to invade through the matrix, compared with the control vector-only cells. Invasive ability was maintained by the tail-less ΔcytoTrop-2 mutant (Fig. 3*B*), with no significant difference in the number of invading clusters with respect to the wt-Trop-2. ΔcytoTrop-2 clusters were smaller than the wt Trop-2 ones at 5 days from seeding, which could reflect differences in cell growth kinetics (see below).

We have previousy shown that Trop-2 tightly interacts at the cell membrane with the ADAM10 metalloproteinase, which in turn leads to activation of Trop-2 via proteolytic cleavage at R87-T88 [13]. ADAM10 has also been shown to be responsible for E-cadherin processing in epithelial cell monolayers, which regulates cell adhesion and sorting [36]. Hence we investigated whether Trop-2 could drive E-cadherin functional inhibition via ADAM10 proteolysis. Western blot analyses of KM12SM tranfectants revealed that Trop-2 induces the release of the E-cadherin 30 kD intracellular domain (Fig. 4*A*). To validate this finding we assessed E-cadherin status in the HT29 colon cancer cell line, which displays a bimodal distribution of Trop-2 expression (Fig. 4*B*). Western blot analyses of distinct HT29 subpopulations selected for low versus high levels of Trop-2 expression confirmed stimulation of E-cadherin cleavage by Trop-2 (Fig. 4*B*). Downregulation of ADAM10 expression by a specific inhibitory shRNA abolished E-cadherin proteolysis in KM12SM/Trop-2 transfectants (Fig. 4*C*), thus indicating ADAM10 as the effector protease of Trop-2-induced E-cadherin shedding. Specificity was confirmed with a second, independent ADAM10 shRNA, which was equally effective in inhibiting Ecadherin processing (Fig. S3*E*).

The E-cadherin/β-catenin complex requires anchoring to the β-actin cytoskeleton for effective cell-cell adhesion [37]. wtTrop-2 severely diminished, and ΔcytoTrop-2 essentially abolished, E-cadherin binding to the actin cytoskeleton (Fig. 3*A*). Mechanistic analysis showed binding of Trop-2 to ezrin, indicating this as a requirement for bridging the Trop-2/E-cadherin/β-catenin complex to the cytoskeleton (Fig. 4*D*).

E-cadherin inactivation leads to activation of the β-catenin transcriptional activity [37]. Such activation requires transit of β-catenin at the cell membrane, for dephosphorylation at S37/T41 [38]. KM12C, pro-metastatic parental KM12SM and KM12SM cells transfected with wtTrop-2, ΔcytoTrop-2 or control vector were analyzed by confocal microscopy for β-catenin levels and localization (Figs.S3*C,F-G*, Figs. 5*A-B,* Table S4*A*). Consistent with a gradient of metastatic competence, the lowest levels of nuclear β-catenin were found in the non-metastatic KM12C < pro-

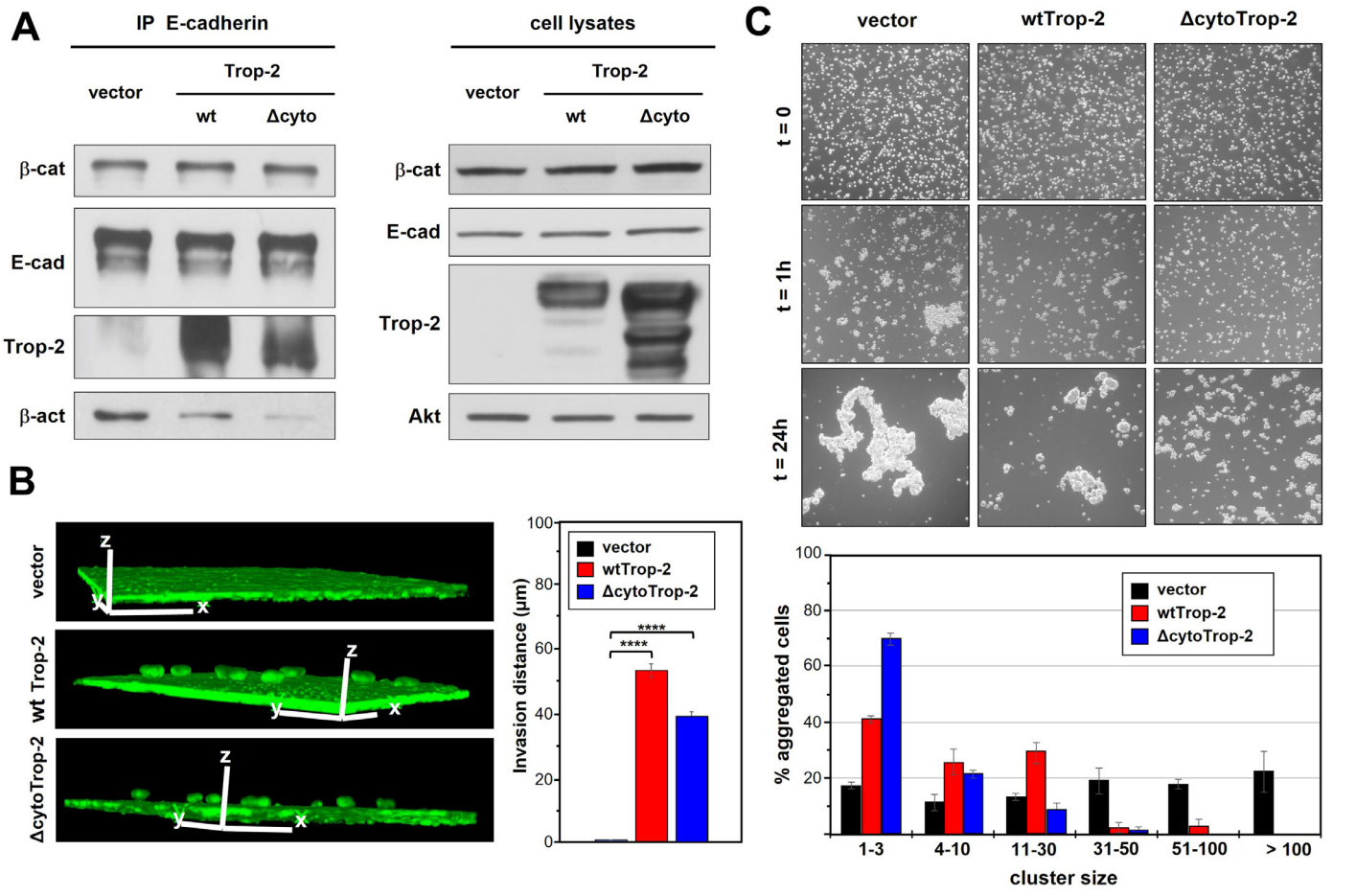

Fig. 3. Trop-2 drives functional inactivation of E-cadherin (*A*) E-cadherin immunoprecipitates from KM12SM transfectants were analysed by Western blotting for β-catenin (β-cat), Trop-2 and β-actin (β-act). E-cadherin (E-cad) was also probed as control (*left*). Corresponding cell lysates were also analysed, with Akt as protein loading control (*right*). (B) Matrigel invasion by KM12SM vector-alone transfectants compared to KM12SM cells expressing either the wtTrop-2 or the ΔcytoTrop-2 at 5 days from seeding (left). Representative images of three independent experiments are shown. The arrow indicates the direction of invasion through the Matrigel layer. Clusters of invading cells are detected only upon overexpression of Trop-2. The total number of invading clusters was not significantly different between wtTrop-2 and ΔcytoTrop-2. The distance of each invading cluster from the matrigel surface along the Z axis was measured; average values for each group are showm in the histogram on the right. (***C***) Cell-cell aggregation in KM12SM transfectants, assessed 1 h and 24 h after seeding on low-attachment plates. Representative phase-contrast images are shown (*top*). Distribution of cell aggregation states after 1 h from seeding was profiled as % of cells in each aggregate class.

metastatic parental KM12SM < wtTrop-2 < ΔcytoTrop-2. Quantitative image analysis showed progressively higher mean values of nuclear/activated β-catenin in vector (mean±SEM 2604 ± 240 SV), wtTrop-2 (mean: 3362±283 SV; P <0.0001 versus control vector) and ΔcytoTrop-2 cells (mean: 4431 ± 196 SV; P<0.0001 versus wtTrop-2) (Fig. S3*G*, Fig. 5*A-B*, Table S4*A*). This demonstrated that β-catenin signaling activation by Trop-2 in colon cancer does not require clustering with a membrane-released Trop-2 cytoplasmic tail [4].

We verified the transcriptional competence of Trop-2-activated β-catenin, using a β-catenin-RE-GFP reporter (Figs. 5*B,C*). GFP-expressing/β-catenin-responsive KM12C cells were 13%. wtTrop-2 increased the percentage of GFP-expressing/β-catenin-responsive KM12C cells to 24%; ΔcytoTrop-2 led them to 28%. As predicted, Trop-2-positive metastatic KM12SM showed higher baseline transcriptional values (47%) than non-metastatic KM12C cells. Overexpression of wtTrop-2 in KM12SM cells led to a further increase of responsive cells to 54% (Figs. 5*B,C*). The highest β-catenin-driven GFP expression was induced by ΔcytoTrop-2 (67% of above-threshold cells).

β-catenin impact on transcription of target genes *in vivo* was assessed. β-catenin regulates genes associated with proliferation, differentiation, migration and angiogenesis. A set of 277 β-catenin target genes in colorectal cancer was retrieved (web.stanford.edu/group/nusselab/cgi-bin/wnt/target_genes; Gene Expression Omnibus database). This included "direct" targets, as defined by the presence of TCF binding sites, and "indirect" targets, as obtained from large-scale β-catenin inactivation screening programs. β-catenin targets included the proto-oncogenes *MYC* and *CCND1*, as well as the genes encoding the basic helix-loop-helix proteins ASCL2 and ITF-2B [39]. This dataset was interrogated in primary tumors and metastases. Most remarkably, essentially no impact of Trop-2 on β-catenin target genes was revealed in primary tumors. Further, β-catenin was found to be downregulated in control, parental KM12SM metastases, with further loss of transcription of β-catenin targets. Massive changes were, on the other hand, revealed in β-catenin target genes in wtTrop-2 metastases (89 target transcripts, 61 genes overall) (Table S4*B*). Notably, control and wtTrop-2-modulated mRNAs showed no overlap, indicating that Trop-2 triggered a distinct control mechanism of metastatic diffusion. The vast majority (50) of

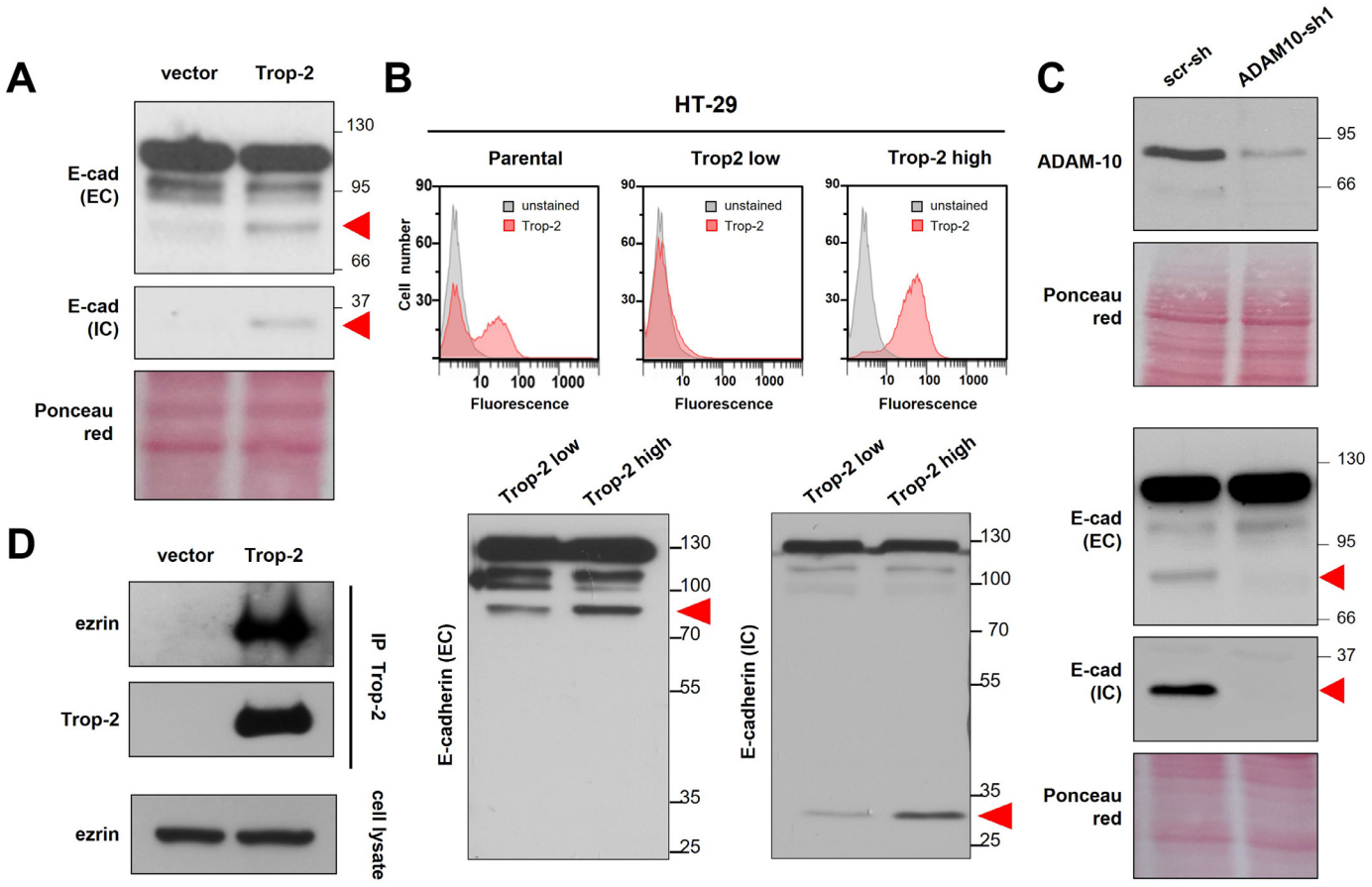

Fig. 4. Trop-2 induces E-cadherin cleavage by ADAM10 (*A*) Western blot analysis of KM12SM/Trop-2 and vector-only transfectants with antibodies against the E-cadherin N-terminal extracellular domain (*top*) or C-terminal cytoplasmic tail (*bottom*). Molecular weight markers are indicated on the right. Red arrowhead: cleaved E-cadherin 80 kD extracellular domain and 30 kD cytoplasmic domain. Ponceau red staining is shown as protein loading control. (B) HT29 colon camcer cell subpopulations were selected from the parental cell line by flow cytometry for low/nihl or high expression of Trop-2 (*top*) and analysed for E-cadherin cleavage by Western blotting as above on full length gels (*bottom*). Uncleaved E-cadherin provide loading control. (*C*) KM12SM/Trop-2 cells were infected with a lentiviral shRNA targeting the ADAM10 transcript (ADAM10-sh1) or with a scramble shRNA (scr-sh) as control. ADAM10 levels (*top*) and E-cadherin cleavage (*middle, bottom*) were revealed by Western blotting as above. Ponceau red staining is shown as protein loading control. (***D***) Trop-2 immunoprecipitates from KM12SM transfectants were analysed by Western blotting for ezrin (*top*). Ezrin levels in corresponding whole lysates are shown (*bottom*).

modulated genes was shared between wtTrop-2 and ΔcytoTrop-2. Marked increased transcription was induced by ΔcytoTrop-2 versus wtTrop-2 in most cases (65/71 genes), consistent with the activated nature of ΔcytoTrop-2 and the aggressiveness of its induced metastases.

The Trop-2/E-cadherin/β-catenin pro-metastatic module in vivo

The Trop-2/E-cadherin/β-catenin pro-metastatic module was validated in colon cancer metastatic xenotransplants. E-cadherin and β-catenin levels were assessed by IHC analysis of matched primary tumor/metastasis pairs. wtTrop-2 KM12SM colon cancer cells showed higher levels of E-cadherin than control, parental cells. Further increase in levels of expression and recruitment to the cell membrane were detected in ΔcytoTrop-2 cells (Fig. S4*A*). Subgroup analyses of primary spleen tumors showed that 45% of controls were devoid of E-cadherin, and only 20% of cases reached high levels of expression. On the other hand, 70% of wtTrop-2 tumors expressed E-Cadherin, 20% of cases reaching high levels. No ΔcytoTrop-2 tumors were devoid of E-cadherin, and almost 60% of cases reached high expression levels (Fig. S4*B*).

In parallel assays, the lowest levels of β-catenin were found in parental KM12SM primary tumors. β-catenin expression increased in liver metastases (Fig. S4*A*). ΔcytoTrop-2 xenotransplants showed a vast increase of β-catenin expressing cells versus control tumors. Correspondingly high β-catenin expression was maintained in matched metastases (Fig. S4*A*). Subgroup analysis for expression of β-catenin showed that 90% of control tumors did not express the protein, and none reached high levels of expression. On the other hand, 10% of wtTrop-2 and 60% of ΔcytoTrop-2 tumors expressed high levels of β-catenin (Fig. S4*B*).

Trop-2 metastatic signalosome dissection

Metastatic diffusion requires resistance to apoptosis, enhanced migration and invasiveness. We modelled the contribution of these mechanisms to the Trop-2-driven metastatic process through global, multi-platform proteomic analyses (Fig. S5, Table S5) and in vitro functional assays (Fig. S6).

Proteomic analysis of wtTrop-2 and ΔcytoTrop-2 metastatic cells showed modulation of RTK signaling, including Erb-B2, PDGFRα, FAK, the FAK-related kinase Pyk2 and PKCs, with Src/FAK-dependent JNK activation (Figure S5, Table S5). wtTrop-2 induced activatory phosphorylation of

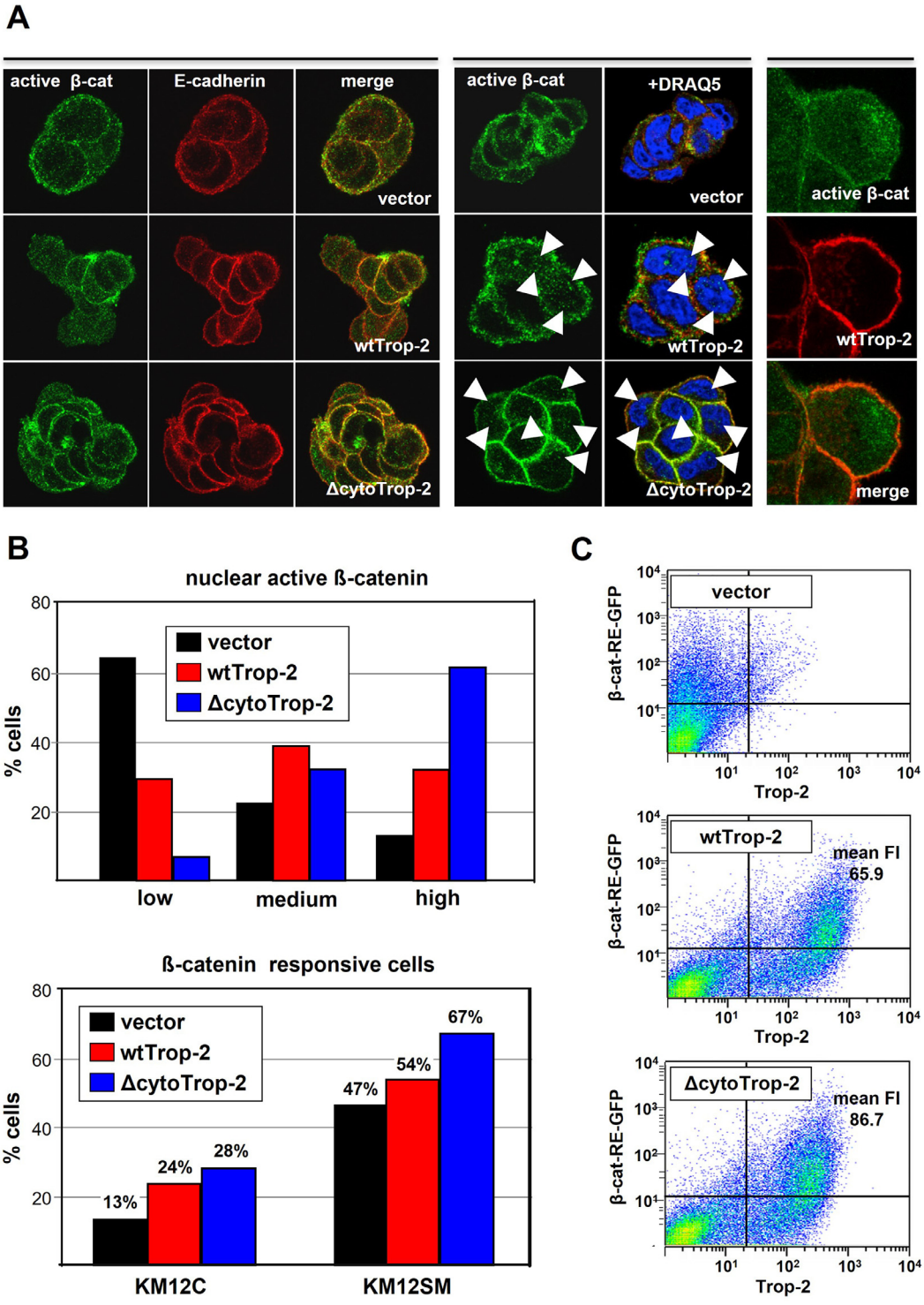

Fig. 5. β-catenin release and activation by Trop-2. Activation of β-catenin transcriptional activity requires transit at the cell membrane and transport to the nucleus. Levels and localization of β-catenin were analyzed in KM12C, KM12SM cells transfected with wtTrop-2, ΔcytoTrop-2 or control vector. (***A***) Confocal microscopy analysis of active unphosphorylated β-catenin in KM12SM transfectants. Active β-catenin colocalization with E-cadherin at the cell membrane (*left*). Nuclear localization (arrowheads): nuclei were identified by counterstaining with DRAQ5 (blue pseudo-color) (*middle*). Co-staining with Trop-2 (*left*) (***B***) Histogram plots of active β-catenin in the nuclei of KM12SM transfectants (see Table S5 for the full dataset) (*top*). Histogram plots of GFP-positive/β-catenin-responsive cells in KM12C non-metastatic and KM12SM metastatic transfectants; subgroup percent values are indicated. (***C***) Flow cytometry analysis of GFP expression in KM12SM cells co-transfected with the pTOPFLASH-EGFP β-catenin-reporter and the empty vector (*top*) or the expression vector for wtTrop-2 (*tmiddle*) or ΔcytoTrop-2 (*bottom*). GFP average fluorescence intensity (FI) is indicated as normalized for Trop-2 transfection efficiency.

Akt at T308 [27]. This was further increased (+80%) by the Δcyto Trop-2 mutant, with Akt-mediated inactivating phosphorylation of Raf-1 (S259) and GSK3α/β (Ser21/Ser9) [27] (Fig. S5*A,B*, Table S5). Trop-2 induced Akt-mediated activation of c-Jun [40] (Table S5). This paralleled claudin-dependent, Akt-driven modulation of the FoxO1/TCF-4/β-catenin transcriptional repressor complex for cell-cell junction assembly [41]. Inactivation/downregulation of Rb contributes to metastatic spreading [42]. Consistent with this, we found reduced levels of Rb in KM12SM cells upon expression of wtTrop-2, and these paralleled activating phosphorylation of PKCε at S729 [43]; Rb levels were further reduced by the Δcyto mutant (Figs. S5*A,B*). Cyclin D1/cdk4 complexes trigger Rb phosphorylation at S807/811 and prevent binding to E2F-1 [44]. Consistent with a model of Trop-2-driven Rb inactivation, these sites were found hyperphosphorylated in KM12SM/Trop-2 (+221.2%) (Table S5).

A large fraction of the 170 proteomic changes which were detected in the Trop-2 signalosome were found to be induced by both wt and ΔcytoTrop-2 (Fig. S5*C*, Table S5*D*). In 23 instances, concordant variations of absolute amounts and/or extent of activatory phosphorylation of signaling proteins were recorded, suggesting these to be core Trop-2-dependent signaling events (Table S5*D*). ΔcytoTrop-2 downregulated absolute amounts and phosphorylation/activation of the p38/MAPK14 cell death inducers and downstream effectors IRAK-1, IRAK-3, TRADD, JAK3, STAT-1 (S727), JAK2 (Y1007-1008) (Table S5). These findings, and the activation of the Ras/Raf/MEK, PTEN/Akt/GSK3, p38/MAPK14, and PKCε (S729) pathways, indicated impact of Trop-2 on pro-survival signaling [1].

A pro-survival role of Trop-2 was validated in *in vitro* functional assays in a range of Trop-2-responsive cell systems (KM12SM colon cancer cells, IGROV-1 ovarian cancer cells, MTE4-14 murine thymic cells; Figs. 6*A-B*) [6,13]. Serum-deprived IGROV-1 and KM12SM/Trop-2 transfectants reached much higher saturation values and survived markedly longer than vector-alone control cells (Figs. S6*A-B*). Activated ΔcytoTrop-2 had a larger impact than wtTrop-2 on cell culture saturation density and survival over time (Fig. S6*A*). Of note, ΔcytoTrop-2 induced slower growth of transfected cells than wtTrop-2 up to 48 hours from seeding, supporting a model of a distinct control of Trop-2 on cell growth versus survival [28], as well as versus invasion (Fig. 3*B*). This was validated in 3D models of metastatic colon cancer, as HCT116 cell spheroids [45] were not appreciably induced to grow by wtTrop-2 (Fig. S6*C*).

Increased cell migration underlie metastatic spreading [1,31]. In wound-healing assays, wtTrop-2 induced effective wound closing (22% of wound area coverage at 6 h versus 14% in parental cells; 78% versus 17% at 24 h in parental cells). ΔcytoTrop-2 further increased cell migration ability, with complete wound closure at 24 h after seeding (Fig. S6*D*).

Selective pressure for Trop-2 expression in metastatic disease

Our findings predicted a critical impact of the Trop-2-driven pro-metastatic program in colon cancer. This was assessed in multiple case series of cancer patients. Proof of principle IHC analysis for protein expression showed progressive induction of Trop-2 from the Trop-2-negative normal colon mucosa, to colon cancer, to metastases, which showed strikingly high expression of Trop-2 (Fig. S7*C*). Trios of normal tissue, primary tumor, and metastasis from individual patients bearing colon, cancer were then analyzed by cDNA dot blot analysis. This showed overexpression of *TROP2* in metastasis in 73% of cases (n = 11) (Fig. S7*A*, Table S6*A*). Such selective pressure for higher expression of *TROP2* in metastasis, supported a driving role of *TROP2* in metastatic diffusion. This applied also to organs and tissues where normal cells do not express *TROP2*, indicating reshaping of gene expression control networks according to a common malignant progression trajectory.

We verified the relevance of such findings in independent cancer patient case series. Analysis of 9 colon cancers and matching metastases indicated upregulation of *TROP2* in metastatic lesions (Fig. S7*B*). Such impact of a global *TROP2* overexpression in metastases was challenged by IHC analysis of a validation case-series of colon normal tissues, primary cancers and matching metastases (n = 48) (Table S6*A-B*). This revealed that Trop-2 was overexpressed in metastases (Fig. S7*D,* Table S6*A-B*), with probability estimates (95% confidence intervals) for higher fractions of metastatic IHC-positive cells than in primary tumors of 88% (CI = 78-97%) of colon carcinomas.

Trop-2 is a predictor of survival in colon cancer patients

We thus went on for assessing Trop-2 impact on colon cancer malignant progression and disease outcome. This was assessed in two independent colon cancer case series. A first patient population (n=80) was examined, with median age of 72 years (range, 30-88) and heterogeneous tumor grading. Evaluable dissected samples indicated lymph-node metastasis at diagnosis in 32 patients, whereas 37 patients were metastasis-free. IHC analysis (Fig. 6A) showed expression of the Trop-2 protein in 65/80 (81.2%) cases. The fraction of Trop-2 expressing cells in the positive cases was up to 100%, with a mean ± S.E. of 41.6% ± 4.0. Among the 80 tumors, 40 (50.0%) exhibited Trop-2 overexpression (Trop-2^{high}). Trop-2^{high} was significantly associated with metastasis to lymph-nodes (P = 0.047) (Table S6*C*). No significant association was detected between Trop-2 expression and other clinicopathologic variables (age, sex, degree of tumor differentiation, tumor staging, tumor invasion).

To quantify the impact of Trop-2 expression on patient survival, a second series of 53 colon cancer patients was surveyed for an extended follow-up time (≈400 months). ROC analysis was applied to compute a Trop-2 positivity threshold according to the 0, 1-criterion. The optimal cut-off parameter for Trop-2 positive expression was 88%. Kaplan-Meier curves showed above-threshold expression as significantly associated with poor OS, with death of 57.1% of patients. Only 37.8% of Trop-2^{low} cases encountered death (P = 0.020) (Fig. 6*B*, Table S6C).

We then went on to assess the impact of coordinate expression of Trop-2 (*TROP2, TACSTD2*), E-cadherin (*CDH1*), β-catenin (*CTNNB1*) on disease outcome and patient survival. Next-generation sequencing analysis of tumor transcriptomes of 597 cases of colon cancer in the TCGA dataset (www.proteinatlas.org) confirmed a negative prognostic impact of *TROP2* mRNA overexpression on patient survival (P =3.67e-3). OS was then analyzed in colon cancer patients (genomics.jefferson.edu/proggene) for coordinate expression of *TROP2, CDH1, CTNNB1* transcripts by DNA microarray analysis (160 cases, with 11 years of follow-up). Significant prognostic impact on patient OS for single-determinant analysis was revealed for *TROP2* (HR = 1.96; P = 0.00058), with no significant impact of *CDH1, CTNNB1* (Fig. 6C). Remarkably, though, coordinate assessment of *TROP2, CDH1, CTNNB1* provided much higher estimates of relative risk on disease outcome and patient survival than any individual parameter alone (HR = 3.85; P =0.0042) (Fig. 6C), consistent with a coordinate impact of the Trop-2-driven module on cancer relapse.

Discussion

In this work we identified Trop-2 as a unique upregulated gene across colon cancer metastasis models and showed for the first time that Trop-2 induces ADAM10 activation for E-cadherin cleavage and inactivation.

E-cadherin has a primary role in establishing cell-cell junctions and maintaining normal tissue architecture, whilst β-catenin takes part to adherent junction complexes and mediates the interactions of E-cadherin with the cytoskeleton by binding to α-catenin [46]. β-actin operates as a scaffold for the assembly of a Ras/Raf/ERK/ezrin complex, which is a key regulator of PI3K/Akt signaling through PI-phosphorylation. As a consequence, E-cadherin requires anchoring to β-actin for function, and

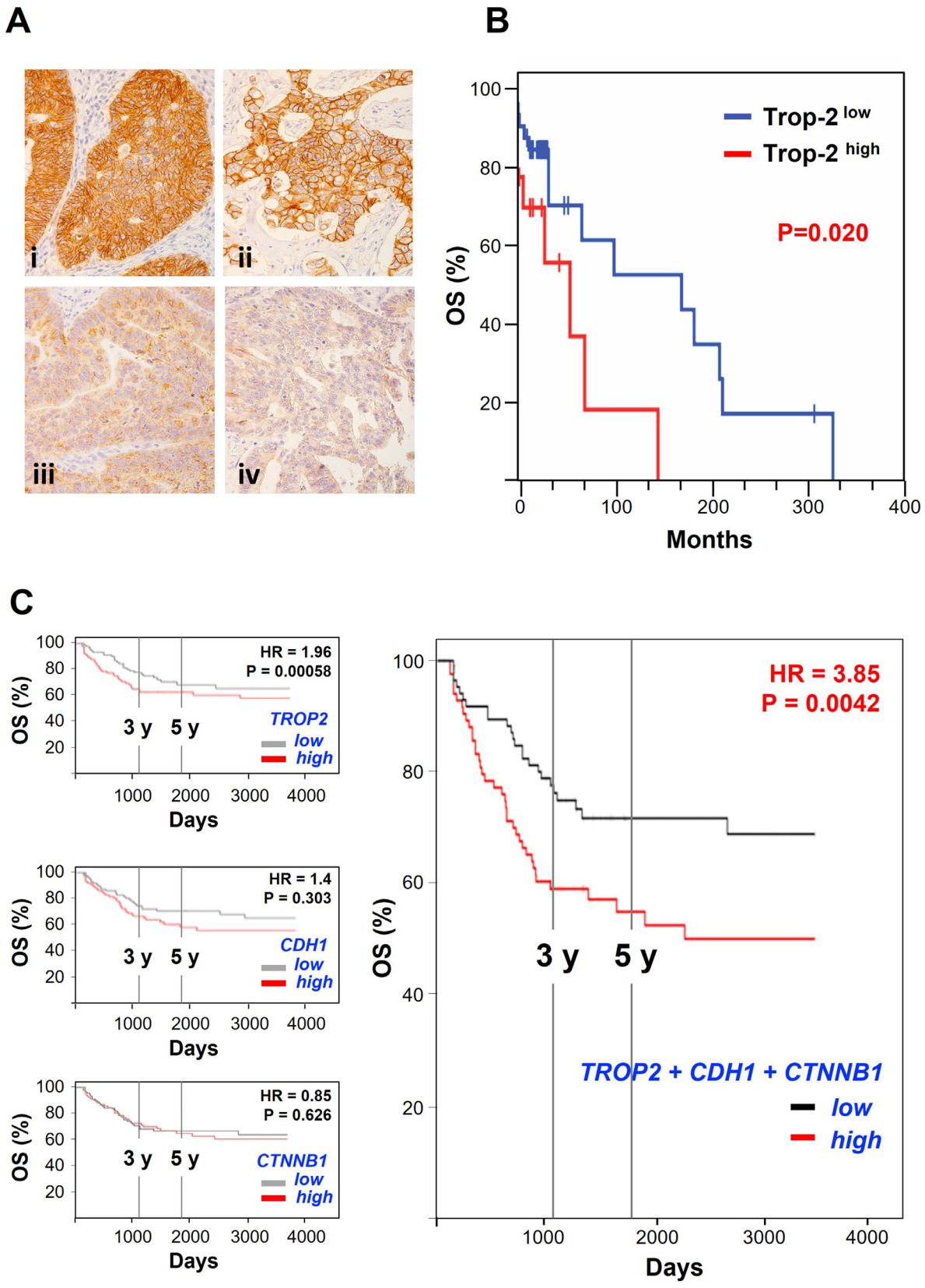

Fig. 6. Impact of the Trop-2/E-cadherin/β-catenin module on colon cancer patient survival. (***A***) Colon cancer IHC staining over a series of cases from high (i) to low (iv) expression of Trop-2 (magnification 40x) (*left*). (***B***) ROC analysis was applied to obtain the Trop-2 positivity threshold according to the 0-1 criterion. The optimal cut-off parameter for Trop-2 positive expression was 88% (Trop-2^{high}: score above the cut-off threshold; Trop-2^{low} score below the threshold). Kaplan-Meier analysis of overall survival (OS) according to Trop-2 expression levels: 57.1% of patients harboring Trop-2^{hi}. (***C***) DNA microarray data from colon cancer patients were pre-processed and meta-analyzed through the KMPlot database (www.kmplot.com). Kaplan-Meier (KM) curves showing the individual impact of *TROP2, CTNNB1* and *CDH1* transcript levels on overall survival (OS) are depicted on the left, while the impact of *TROP2, CTNNB1* and *CDH1* coexpression is shown on the right. Vertical bars are shown for assessment at 3 and 5 years from diagnosis.

inhibition of tumor progression, through retention of β-catenin [46]. On the opposite side, release of β-catenin leads to translocation to the nucleus, and activation as a transcription factor on target genes, including those that promote cell proliferation, differentiation, migration and angiogenesis [46].

In colon cancer experimental models, we revealed a gradient of metastatic competence, with the lowest levels of nuclear β-catenin observed in the Trop-2-nil non-metastatic KM12C colon cancer cells, higher levels measured in the Trop-2-prone pro-metastatic KM12SM cells, and the highest levels reached in the metastatic wtTrop-2 and ΔcytoTrop-2 KM12SM cells. This paralleled the ability of wtTrop-2 and ΔcytoTrop-2 to induce ADAM10 cleavage of E-cadherin and disanchoring from the cytoskeleton, which then led to a corresponding loss of cell-cell aggregation. The transcriptional capacity of the released β-catenin was demonstrated in β-catenin-RE-GFP reporter assays *in vitro*. This was paralleled by massive induction of β-catenin transcriptional target genes in wtTrop-2 and ΔcytoTrop-2-driven metastases *in vivo*. No trace of these changes was found in control metastasis, indicating that wtTrop-2 triggers a unique mechanism of metastatic dissemination.

E-cadherin loss has been widely considered to be required for EMT-dependent tissue invasion [47]. However, our findings showed no transcriptional downregulation of the *CDH1* gene in Trop-2-activated cells, nor expression of EMT transcription factors that suppress the transcription of epithelial differentiation markers. Instances of incomplete/graded EMT have been recognized [25,31,47,48]. Our findings add a novel turn to these scenarios, whereby Trop-2 induced E-cadherin cleavage and inactivation, as mediated by ADAM10. Unsurprisingly, this associated to retention of epithelial differentiation biomarkers, high levels of β-catenin and of β-catenin transcriptional targets. Our findings thus appear to recapitulate frequent surgical pathology assessments, that show inactivation/disarray of E-cadherin in aggressive tumors [49], for release of transcription-versed β-catenin into the cytoplasm of cancer cells and association to tumor progression [37], in the apparent absence of loss of epithelial differentiation.

IHC analysis of distinct colon cancer case series showed that up to 88% of the tumors exhibited Trop-2 overexpression, and that overexpressed Trop-2 was significantly associated with metastasis to lymph nodes. An extended follow-up (≈400 months) of metastatic colon cancer patients, showed that high Trop-2 expression correlated with poor OS, and with fatal events in 57.1% of highly-expressing cases. Corresponding findings were obtained by transcriptomic analysis of independent colon cancer case series, where overexpression of Trop-2, β-catenin and E-cadherin showed heavy impact on patient survival. Notably, this impact was not matched by any of the risk factors taken individually, suggesting a pivotal pathological role of the Trop-2-driven module on colon cancer progression. Of note, the anti-Trop-2 mAb Sacituzumab govitecan-hziy was shown to be effective in metastatic breast cancer patients [14-17] and was granted accelerated FDA approval (www.fda.gov/drugs/drug-approvals-and-databases/drug-trial-snapshot-trodelvy). Our findings provide ground for potential major relevance of Trop-2 as a target in metastatic colon cancer.

Author contributions

E.G., M.T., V.R. R.T., G.V., M.C., K.B., R.Z., P.S., and S.A. performed the cell biology tests, biochemical analyses and *in vivo* assays. R.d.L. and U.H.W. performed the DNA macroarray and microarray analyses for tumor cell line profiling. M.T. identified the gene interaction networks. R.L., D.F.A., R.D., M.T.R., A.P., P.Q., M.P., E.B., D.A., G.P., C.D.L., M.P. and X.-F.S. collected the human tumor samples, constructed the tissue microarrayS and performed the IHC analyses. S.B., A.C., P.D.R., A.M., V.G. and S.A. performed the quantitative meta-analyses of surgical pathology and *in silico* data. L.A. and R.L. performed the statistical analyses. E.G., M.T. and S.A. planned the studies, evaluated the data, and wrote the paper.

Emanuela Guerra: Conceptualization, Investigation, Formal analysis, Data curation, Writing – Original draft, Writing – review & editing. Visualization.

Marco Trerotola: Conceptualization, Investigation, Formal analysis, Writing – Original draft, Writing – review & editing. Visualization, Funding acquisition.

Valeria Relli: Investigation, Formal analysis.

Rossano Lattanzio: Resources, Investigation, Formal analysis.

Romina Tripaldi: Investigation, Formal analysis.

Giovanna Vacca: Investigation, Formal analysis.

Martina Ceci: Investigation, Formal analysis..

Khouloud Boujnah: Investigation, Formal analysis, Data curation.

Valeria Garbo: Investigation, Formal analysis, Data curation.

Antonino Moschella: Investigation, Formal analysis, Data curation.

Romina Zappacosta: Investigation, Formal analysis.

Pasquale Simeone: Investigation, Formal analysis, Data curation.

Robert de Lange: Resources, Formal analysis.

Ulrich H. Weidle: Resources, Formal analysis.

Maria Teresa Rotelli: Resources, Formal analysis.

Arcangelo Picciariello: Resources, Formal analysis.

Raffaella Depalo: Resources, Formal analysis.

Patrizia Querzoli: Resources, Formal analysis.

Massimo Pedriali: Resources, Formal analysis.

Enzo Bianchini: Resources, Formal analysis.

Domenico Angelucci: Resources, Formal analysis.

Giuseppe Pizzicannella: Resources, Formal analysis.

Carla Di Loreto: Resources, Formal analysis.

Mauro Piantelli: Resources, Investigation, Formal analysis.

Laura Antolini: Investigation, Formal analysis.

Xiao-Feng Sun: Resources, Formal analysis.

Donato F. Altomare: Resources, Formal analysis.

Saverio Alberti: Conceptualization, Formal analysis, Writing – Original draft, Writing – review & editing. Visualization, Supervision, Project administration, Funding acquisition

Competing interest

The authors declare the following financial interests/personal relationships which may be considered as potential competing interests. EG is an inventor in patents WO201687651 and WO201784763, and a partner in Mediterranea Theranostic Srl. MT is an inventor in patent WO201784763. SA is an inventor in patents WO201089782, WO201687651 and WO201784763, and is founder and CEO of Oncoxx Biotech Srl and Mediterranea Theranostic Srl. VR was an employee of Oncoxx Biotech Srl. RdL and UHW were employees of Roche Diagnostics GmbH. PS is an inventor in a patent application under consideration (EP3546948). The sponsors had no role in the design and conduct of this study, nor in the collection, analysis and interpretation of the data, nor in the preparation, review or approval of the manuscript.

Acknowledgments

We thank A.M. Cherubino and W. Dietmaier for support in the pathological analysis of tumor samples, U. Brehm, H. Schindler, R. La Sorda for help during the course of this work. Support was provided by grants of Fondazione of the Cassa di Risparmio della Provincia di Chieti, the Compagnia di San Paolo (Grant 2489IT), the Italian Ministry of Development (MI01_00424), Region Abruzzo (POR FESR) C78C14000100005, and Oncoxx Biotech (Italian Ministry of University and Research, Smart Cities and Communities SCN_00558). M.T. was supported

by the Programma Per Giovani Ricercatori "Rita Levi Montalcini", Italian Ministry of University and Research (Grant PGR12I7N1Z).

Supplementary materials

Supplementary material associated with this article can be found, in the online version, at doi:10.1016/j.neo.2021.07.002.

References

[1] Hanahan D, Weinberg RA. Hallmarks of cancer: the next generation. *Cell* 2011;**144**:646–74.

[2] Dongre A, Weinberg RA. New insights into the mechanisms of epithelial–mesenchymal transition and implications for cancer. *Nature Reviews Molecular Cell Biology* 2019;**20**:69–84.

[3] Amit I, Citri A, Shay T, Lu Y, Katz M, Zhang F, Tarcic G, Siwak D, Lahad J, Jacob-Hirsch J, et al. A module of negative feedback regulators defines growth factor signaling. *Nat Genet* 2007;**39**:503–12.

[4] Stoyanova T, Goldstein AS, Cai H, Drake JM, Huang J, Witte ON. Regulated proteolysis of Trop2 drives epithelial hyperplasia and stem cell self-renewal via beta-catenin signaling. *Genes Dev* 2012;**26**:2271–85.

[5] Trerotola M, Rathore S, Goel HL, Li J, Alberti S, Piantelli M, Adams D, Jiang Z, Languino LR. CD133, Trop-2 and alpha2beta1 integrin surface receptors as markers of putative human prostate cancer stem cells. *Am J Transl Res* 2010;**2**:135–44.

[6] Trerotola M, Cantanelli P, Guerra E, Tripaldi R, Aloisi AL, Bonasera V, Lattanzio R, de Lange R, Weidle UH, Piantelli M. Up-regulation of Trop-2 quantitatively stimulates human cancer growth. *Oncogene* 2013;**32**:222–33.

[7] Trerotola M, Jernigan D, Liu Q, Siddiqui J, Fatatis A, Languino L. Trop-2 promotes prostate cancer metastasis by modulating β1 integrin functions. *Cancer Res* 2013;**73**:3155–67.

[8] Hsu E-C, Rice MA, Bermudez A, Marques FJG, Aslan M, Liu S, Ghoochani A, Zhang CA, Chen Y-S, Zlitni A, et al. Trop2 is a driver of metastatic prostate cancer with neuroendocrine phenotype via PARP1. *Proceedings of the National Academy of Sciences* 2020;**117**:2032.

[9] Tang G, Tang Q, Jia L, Chen Y, Lin L, Kuai X, Gong A, Feng Z. TROP2 increases growth and metastasis of human oral squamous cell carcinoma through activation of the PI3K/Akt signaling pathway. *International journal of molecular medicine* 2019;**44**:2161–70.

[10] Li X, Teng S, Zhang Y, Zhang W, Zhang X, Xu K, Yao H, Yao J, Wang H, Liang X. TROP2 promotes proliferation, migration and metastasis of gallbladder cancer cells by regulating PI3K/AKT pathway and inducing EMT. *OncoTarget* 2017.

[11] Zhao W, Kuai X, Zhou X, Jia L, Wang J, Yang X, Tian Z, Wang X, Lv Q, Wang B, et al. Trop2 is a potential biomarker for the promotion of EMT in human breast cancer. *Oncol Rep* 2018;**40**:759–66.

[12] Zhao W, Jia L, Kuai X, Tang Q, Huang X, Yang T, Qiu Z, Zhu J, Huang J, Huang W, et al. The role and molecular mechanism of Trop2 induced epithelial-mesenchymal transition through mediated beta-catenin in gastric cancer. *Cancer Med* 2019;**8**:1135–47.

[13] Trerotola M, Guerra E, Ali Z, Aloisi AL, Ceci M, Simeone P, Acciarito A, Zanna P, Vacca G, D'Amore A, et al. Trop-2 cleavage by ADAM10 is an activator switch for cancer growth and metastasis. *Neoplasia* 2021;**23**:415–28.

[14] Bardia A, Mayer IA, Diamond JR, Moroose RL, Isakoff SJ, Starodub AN, Shah NC, O'Shaughnessy J, Kalinsky K, Guarino M, et al. Efficacy and Safety of Anti-Trop-2 Antibody Drug Conjugate Sacituzumab Govitecan (IMMU-132) in Heavily Pretreated Patients With Metastatic Triple-Negative Breast Cancer. *J Clin Oncol* 2021;**35**:2141–8.

[15] Bardia A, Hurvitz SA, Tolaney SM, Loirat D, Punie K, Oliveira M, Brufsky A, Sardesai SD, Kalinsky K, Zelnak AB, et al. Sacituzumab Govitecan in Metastatic Triple-Negative Breast Cancer. *N Engl J Med* 2021;**384**:1529–41.

[16] Thomas A, Pommier Y. Targeting Topoisomerase I in the Era of Precision Medicine. *Clin Cancer Res* 2019;**25**:6581–9.

[17] Bardia A, Mayer IA, Vahdat LT, Tolaney SM, Isakoff SJ, Diamond JR, O'Shaughnessy J, Moroose RL, Santin AD, Abramson VG, et al. Sacituzumab Govitecan-hziy in Refractory Metastatic Triple-Negative Breast Cancer. *N Engl J Med* 2019;**380**:741–51.

[18] Morikawa K, Walker SM, Nakajima M, Pathak S, Jessup JM, Fidler IJ. Influence of organ environment on the growth, selection, and metastasis of human colon carcinoma cells in nude mice. *Cancer Res* 1988;**48**:6863–71.

[19] Brattain MG, Fine WD, Khaled FM, Thompson J, Brattain DE. Heterogeneity of malignant cells from a human colonic carcinoma. *Cancer Res* 1981;**41**:1751–6.

[20] El Sewedy T, Fornaro M, Alberti S. Cloning of the murine *Trop2* gene: conservation of a PIP2-binding sequence in the cytoplasmic domain of Trop-2. *Int J Cancer* 1998;**75**:324–30.

[21] Romero-Calvo I, Ocón B, Martínez-Moya P, Suárez MD, Zarzuelo A, Martínez-Augustin O, de Medina FS. Reversible Ponceau staining as a loading control alternative to actin in Western blots. *Anal Biochem* 2010;**401**:318–320.

[22] Trerotola M, Li J, Alberti S, Languino LR. Trop-2 inhibits prostate cancer cell adhesion to fibronectin through the β1 integrin-RACK1 axis. *J Cell Physiol* 2012;**227**:3670–7.

[23] Scott RW, Hooper S, Crighton D, Li A, Konig I, Munro J, Trivier E, Wickman G, Morin P, Croft DR, et al. LIM kinases are required for invasive path generation by tumor and tumor-associated stromal cells. *J Cell Biol* 2010;**191**:169–185.

[24] Alberti S, Nutini M, Herzenberg LA. DNA methylation prevents the amplification of TROP1, a tumor associated cell surface antigen gene. *Proc Natl Acad Sci USA* 1994;**91**:5833–7.

[25] Aceto N, Bardia A, Miyamoto DT, Donaldson MC, Wittner BS, Spencer JA, Yu M, Pely A, Engstrom A, Zhu H, et al. Circulating tumor cell clusters are oligoclonal precursors of breast cancer metastasis. *Cell* 2014;**158**:1110–22.

[26] Cernat L, Blaj C, Jackstadt R, Brandl L, Engel J, Hermeking H, Jung A, Kirchner T, Horst D. Colorectal cancers mimic structural organization of normal colonic crypts. *PLoS One* 2014;**9**:e104284.

[27] Guerra E, Trerotola M, Tripaldi R, Aloisi AL, Simeone P, Sacchetti A, Relli V, A DA, La Sorda R, Lattanzio R, et al. Trop-2 induces tumor growth through Akt and determines sensitivity to Akt inhibitors. *Clin Cancer Res* 2016;**22**:4197–205.

[28] Guerra E, Trerotola M, Aloisi AL, Tripaldi R, Vacca G, La Sorda R, Lattanzio R, Piantelli M, Alberti S. The Trop-2 signalling network in cancer growth. *Oncogene* 2013;**32**:1594–600.

[29] Guerra E, Cimadamore A, Simeone P, Vacca G, Lattanzio R, Botti G, Gatta V, D'Aurora M, Simionati B, Piantelli M, et al. p53, cathepsin D, Bcl-2 are joint prognostic indicators of breast cancer metastatic spreading. *BMC Cancer* 2016;**16**:649.

[30] Kohn KW, Zeeberg BM, Reinhold WC, Pommier Y. Gene expression correlations in human cancer cell lines define molecular interaction networks for epithelial phenotype. *PLoS One* 2014;**9**:e99269.

[31] Derynck R, Weinberg RA. *EMT and Cancer: More Than Meets the Eye* Dev Cell 2019;**49**:313–16.

[32] Brabletz T. To differentiate or not - routes towards metastasis. *Nat Rev Cancer* 2012.

[33] Zanna P, Trerotola M, Vacca G, Bonasera V, Palombo B, Guerra E, Rossi C, Lattanzio R, Piantelli M, Alberti S. Trop-1 Are Conserved Growth Stimulatory Molecules That Mark Early Stages of Tumor Progression. *Cancer* 2007;**110**:452–64.

[34] Cavallaro U, Christofori G. Cell adhesion and signalling by cadherins and Ig-CAMs in cancer. *Nat Rev Cancer* 2004;**4**:118–32.

[35] Scott RW, Crighton D, Olson MF. Modeling and imaging 3-dimensional collective cell invasion. *J Vis Exp* 2011.

[36] Solanas G, Cortina C, Sevillano M, Batlle E. Cleavage of E-cadherin by ADAM10 mediates epithelial cell sorting downstream of EphB signalling. *Nat Cell Biol* 2011;**13**:1100–7.

[37] Borghi N, Sorokina M, Shcherbakova OG, Weis WI, Pruitt BL, Nelson WJ, Dunn AR. E-cadherin is under constitutive actomyosin-generated tension that is increased at cell-cell contacts upon externally applied stretch. *Proc Natl Acad Sci U S A* 2012;**109**:12568–73.

[38] van Noort M, Meeldijk J, van der Zee R, Destree O, Clevers H. Wnt signaling controls the phosphorylation status of beta-catenin. *J Biol Chem* 2002;**277**:17901–5.

[39] Zhao H, He L, Yin D, Song B. Identification of beta-catenin target genes in colorectal cancer by interrogating gene fitness screening data. *Oncol Lett* 2019;**18**:3769–77.

[40] Vivanco I, Palaskas N, Tran C, Finn SP, Getz G, Kennedy NJ, Jiao J, Rose J, Xie W, Loda M, et al. Identification of the JNK signaling pathway as a functional target of the tumor suppressor PTEN. *Cancer Cell* 2007;**11**:555–69.

[41] Taddei A, Giampietro C, Conti A, Orsenigo F, Breviario F, Pirazzoli V, Potente M, Daly C, Dimmeler S, Dejana E. Endothelial adherens junctions control tight junctions by VE-cadherin-mediated upregulation of claudin-5. *Nat Cell Biol* 2008;**10**:923–34.

[42] Arima Y, Hayashi H, Sasaki M, Hosonaga M, Goto TM, Chiyoda T, Kuninaka S, Shibata T, Ohata H, Nakagama H, et al. Induction of ZEB proteins by inactivation of RB protein is key determinant of mesenchymal phenotype of breast cancer. *J Biol Chem* 2012;**287**:7896–906.

[43] Garczarczyk D, Toton E, Biedermann V, Rosivatz E, Rechfeld F, Rybczynska M, Hofmann J. Signal transduction of constitutively active protein kinase C epsilon. *Cell Signal* 2009;**21**:745–52.

[44] Kato J, Matsushime H, Hiebert SW, Ewen ME, Sherr CJ. Direct binding of cyclin D to the retinoblastoma gene product (pRb) and pRb phosphorylation by the cyclin D-dependent kinase CDK4. *Genes Dev* 1993;**7**:331–42.

[45] Merenda A, Fenderico N, Maurice MM. Wnt Signaling in 3D: Recent Advances in the Applications of Intestinal Organoids. *Trends in Cell Biology* 2020;**30**:60–73.

[46] Brembeck FH, Rosário M, Birchmeier W. Balancing cell adhesion and Wnt signaling, the key role of β-catenin. *Current Opinion in Genetics & Development* 2006;**16**:51–9.

[47] Yang J, Antin P, Berx G, Blanpain C, Brabletz T, Bronner M, Campbell K, Cano A, Casanova J, Christofori G, et al. Guidelines and definitions for research on epithelial–mesenchymal transition. *Nature Reviews Molecular Cell Biology* 2020;**21**:341–52.

[48] Aiello NM, Maddipati R, Norgard RJ, Balli D, Li J, Yuan S, Yamazoe T, Black T, Sahmoud A, Furth EE, et al. EMT Subtype Influences Epithelial Plasticity and Mode of Cell Migration. *Dev Cell* 2018;**45**:681–95 e684.

[49] Querzoli P, Coradini D, Pedriali M, Boracchi P, Ambrogi F, Raimondi E, La Sorda R, Lattanzio R, Rinaldi R, Lunardi M, et al. An immunohistochemically positive E-cadherin status is not always predictive for a good prognosis in human breast cancer. *Br J Cancer* 2010;**103**:1835–9.